Copy 615

62 72200

NASA TM X-376

[redacted]

[redacted]

NASA TM X-376

TECHNICAL MEMORANDUM

X-376

THE AERODYNAMIC CHARACTERISTICS OF SOME LIFTING BODIES

By David H. Dennis and George G. Edwards

Ames Research Center
Moffett Field, Calif.

CLASSIFICATION CHANGED TO UNCLASSIFIED
By Authority of 10-7053 Date 9-15-70

FACILITY FORM 602

N70-77383 (ACCESSION NUMBER)	(THRU)
18 (PAGES)	None (CODE)
(NASA CR OR TMX OR AD NUMBER)	(CATEGORY)

Declassified by authority of NASA
Classification Change Notices No. 207
Dated ** 11-30-70

[redacted]

[redacted]

NATIONAL AERONAUTICS AND SPACE ADMINISTRATION

WASHINGTON September 1960

[redacted]

[redacted]

NATIONAL AERONAUTICS AND SPACE ADMINISTRATION

TECHNICAL MEMORANDUM X-376

THE AERODYNAMIC CHARACTERISTICS OF SOME LIFTING BODIES*

By David H. Dennis and George G. Edwards

SUMMARY

Lifting bodies having low fineness ratio and hypersonic lift-drag ratios of about 0.5 are discussed briefly. Results of a recent investigation of relatively slender blunt half-cones show hypersonic maximum lift-drag ratios of about 1.5. It is demonstrated that a blunt half-cone with a half-cone angle of 13° can be modified to form an entry vehicle having the capability of a conventional landing while retaining a hypersonic lift-drag ratio of about 1.5. Some preliminary static stability and control results are presented.

INTRODUCTION

Studies of vehicles suitable for entry into the earth's atmosphere have covered a wide range of configurations including nonlifting and lifting bodies and a variety of winged shapes. This paper presents some of the work performed at Ames Research Center on the lifting-body portion of the spectrum of possible entry vehicles. To be discussed are bodies consisting of portions of blunt cones. The first two bodies, to be discussed only briefly, have lift-drag ratios of about 0.5 and have, therefore, rather limited maneuvering capability during entry. The third configuration, a relatively slender, blunt half-cone, has considerably greater maneuverability due to its lift-drag ratio of about 1.5 at hypersonic speeds. The aerodynamic characteristics of this basic half-cone shape are shown. Modifications made to provide for adequate subsonic characteristics and for control throughout the speed range are described and test results are presented.

---

*[redacted] Unclassified

[redacted]

SYMBOLS

C_L	lift coefficient
C_l	rolling-moment coefficient
C_m	pitching-moment coefficient
$C_{m,o}$	pitching-moment coefficient at $C_L = 0$
C_n	yawing-moment coefficient
C_{l_β}	effective dihedral parameter, per deg
C_{m_α}	static longitudinal stability parameter, per deg
C_{n_β}	static directional stability parameter, per deg
L/D	lift-drag ratio
$(L/D)_{max}$	maximum lift-drag ratio
l	body length
M	Mach number
R	Reynolds number
α	angle of attack, deg
δ	deflection of control surface, deg
δ_E	elevon deflection, deg
δ_Y	yaw-flap deflection, deg

L
1
0
9
3

DISCUSSION

Bodies Having Low Lift-Drag Ratios

Results for a body having a low lift-drag ratio were presented in reference 1. The body shape tested and some of the measured aerodynamic characteristics are reviewed briefly in figures 1 and 2. Figure 1 shows a three-view sketch of the body, which is essentially a blunt 30° half-cone with four low-aspect-ratio flaps for control. The aerodynamic characteristics of this particular configuration have been determined over a wide speed range from tests in several wind tunnels. Some of the measured and estimated aerodynamic characteristics are shown in figure 2. At the left of figure 2 is the variation with Mach number of maximum trimmed lift-drag ratio. The experimentally determined lift-drag ratio is slightly more than 0.5 at the higher Mach numbers. This value agrees well with the theoretical value of 0.56 for $M = \infty$ that was calculated with the use of impact theory. Also shown (fig. 2) as functions of Mach number are the experimentally determined static longitudinal- and lateral-directional stability derivatives along with estimated values of these characteristics from impact theory. The particular points to be observed are as follows: First, the configuration was statically stable about the pitch and yaw axes and had positive dihedral effect; second, the stability levels were relatively insensitive to variations of angle of attack near the attitude for $(L/D)_{max}$ or to variations of Mach number at the higher supersonic speeds; and, third, the performance and stability at high speeds were well predicted in this case with the use of simple impact-theory calculations.

L
1
0
9
3

Studies have continued on other lifting bodies having lift-drag ratios of about 0.5 at hypersonic speeds. An investigation has been initiated recently on another cone-segment-type body. The particular shape, shown in figure 3, is approximately one-sixth of a blunt cone. The cone half-angle is 58° and, at the attitude where the estimated value of L/D is 0.5, the cone axis is alined with the stream. With the high incidence angle of the conical surface, this body would experience higher heating rates over a relatively smaller surface than the 30° half-cone. Thus, this shape would be more attractive for use with ablation-type thermal protection.

Initial experimental results obtained with the cone-segment body of the type presented in figure 3 show that the measured value of L/D at the design attitude agrees with the estimated value of 0.5. The body is longitudinally stable about its center of volume but it is considerably out of trim in the present configuration. Also, as in the case of most lifting configurations operating at high angles of attack, this shape has the disadvantage of having a negative lift-curve slope. Further analysis and testing will be required to establish the desirability of employing body shapes of this type.

Returning again to the blunt half-cone shapes, the generally favorable aerodynamic properties of the 30° blunt half-cone indicated that study of other bodies of this type might prove to be of interest.

Since a lift-drag ratio of 0.5 at hypersonic speeds provides for relatively limited maneuverability, it was desired that further study be directed toward bodies having higher lift-drag ratios.

Basic Body Having High Lift-Drag Ratio

One approach to obtaining higher values of L/D that was studied briefly was the addition of a small wing to the top surface of the 30° half-cone. Lift-drag ratio at hypersonic speeds was increased by this means to a value of about 0.9. Another approach for increasing L/D, by increasing body slenderness, was more extensively investigated both analytically and experimentally for half-cone angles in the range from 10° to 20°. Of the more slender half-cone shapes, one was selected for the detailed study to be discussed herein. This configuration, shown in figure 4, has a half-cone angle of 13°. According to estimates, the value of L/D for this shape at infinite Mach number is about 1.5 and is 1.25 to 1.33 at Mach numbers from 3 to 5. This lift-drag ratio is sufficient to provide for lateral ranges during entry from satellite orbit of about 1,000 nautical miles, or about 5 times that available to a vehicle with a value of L/D of 0.5. With this lateral range, incidentally, it is possible to return to a launch point after one circumnavigation of the earth for most orbits attained by launching in the continental United States.

L
1
0
9
3

The longitudinal characteristics of this shape were measured at supersonic speeds and results obtained at a test Mach number of 5 are presented in figure 5. The circled data points, as well as the dashed lines indicating the estimated variations of lift-drag ratio and pitching-moment coefficient with lift coefficient, are for the basic 13° blunt half-cone. The theory used was a combination of impact theory on the nose and on the conical surface and shock-expansion theory over the top surface. The base drag was obtained from the assumption that the base-pressure coefficient was 0.7 of the vacuum-pressure coefficient. As in the case of the 30° half-cone, the relatively simple analytical methods provide a fairly good estimate of lift-drag ratio and of the variation of C_m with C_L, at least at the Mach numbers of these tests. However, the body trims near $C_L = 0$ rather than near $(L/D)_{max}$ as estimated. Trim nearer $(L/D)_{max}$ can be achieved by modification of the lower afterportion of the conical surface as shown on the sketch at the top of figure 5 and by the triangular data points. The stability is essentially unchanged but the trim point is at a lift-drag ratio of approximately 1.2. The lower-surface modification increased the value of $(L/D)_{max}$ slightly.

Forces and moments on this body were also measured at low speeds to determine if such a body shape would be flyable at subsonic speeds at the conclusion of an entry maneuver. Figure 6 shows the measured variations of pitching-moment coefficient and lift-drag ratio with lift coefficient at a Mach number of 0.25. It may be seen that the body is neutrally stable and has a maximum lift-drag ratio of only 1.7. The low lift-drag ratio is due to the large base area (47 percent of the planform area) and to the poor pressure recovery at the base.

Modified Body Having High Lift-Drag Ratio

L1093

In order to improve the rather poor subsonic characteristics just described, an investigation of the flow characteristics and the effects of body modifications was conducted in the Ames 12-foot pressure tunnel. Much of this program pertained to boattailing the body in an effort to reduce the base area, to improve the lifting characteristics of the upper surface, and to promote a positive $C_{m,o}$. Some typical body shapes and test results are presented in figures 7 and 8. Figure 7 shows three lifting bodies: the blunt half-cone, one of the boattailed bodies, and a vehicle with the same boattailed body with canopy, vertical surfaces, elevons, and a trailing-edge flap. The large influence of modifying the rear portion of the body on the lift-drag ratios can be seen in figure 8. Base area was reduced from 47 percent to 17 percent of the planform area and the improved flow increased the base-pressure coefficient from -0.24 to about 0. The configuration with canopy and stabilizing surfaces shows even higher lift-drag ratios than the modified body alone. This effect has been attributed to a favorable end-plate effect due to adding the vertical surfaces and to the increased aspect ratio due to adding elevons. Note that the pitching-moment curve for the complete configuration is nearly linear and, for these data, shows trim at a lift coefficient of 0.55.

Some effects of variations in canopy shape were also determined during the course of the investigation at subsonic speeds. The original spherical canopy is shown in figure 9 and a faired canopy is shown in figure 10. It was anticipated that the faired canopy might improve the lift as well as provide additional volume; however, the results were quite adverse. The faired canopy interfered with the strong vortex flows that originate at the leading edges of the upper surface so that at some angle of attack, the vortices were diverted outward to impinge on the vertical surfaces and roll controls. The resulting moment characteristics were nonlinear and the lift-drag ratio was reduced. It appears, then, that the canopy should not extend to the leading edges of the top surfaces of the body.

The body modifications and the addition of stabilizing fins and elevons resulted in relatively good subsonic stability and performance characteristics, and conventional landing capability is indicated. To study means for providing for control of this type of configuration throughout the speed range, the afterportion of the study configuration was modified further to include pitch and yaw flaps in addition to the elevons which are primarily for roll control. These modifications are illustrated in figures 11 and 12. Figure 11 shows the configuration just discussed, without elevons; the revised configuration is shown in figure 12. An objective was to provide controls which would have a minimum of cross coupling. The sides of the body were flattened and faired into the vertical stabilizer surface to provide for the yaw controls. Similarly, the bottom was flattened and a pair of pitch controls was provided. These modifications affected only the rear one-third of the body and the resulting body lines were not as conducive to good pressure recovery at the base as those of the original model. The base area of the revised configuration is 22 percent of the planform area compared with 17 percent for the previous configuration. Most of this increase is represented in increased base area of the vertical surfaces and elevons which were thickened to relieve the heating problems at their leading edges.

L1093

Figure 13 shows the revised configuration with simulated landing gear. Typical preliminary results obtained on this model are presented in figure 14. Pitching-moment coefficient and lift-drag ratio as functions of lift coefficient are shown. It is evident that the landing gear had little effect. The modifications increased minimum drag considerably and the revised configuration does not exhibit the high lift-drag ratios at low lift coefficients that were characteristic of the earlier model. However, the lift-drag ratios are about the same as before at the higher lift coefficients, and the pitch characteristics remain good. For example, the lift-drag ratio is 3.2 at a trimmed lift coefficient of 0.6 with a static margin of 9.5 percent (center of gravity at 55 percent of the body length). With the development of improved low L/D landing techniques (see, e.g., refs. 2 and 3), it is felt that a vehicle such as this would be capable of performing a conventional landing.

Some of the characteristics of this revised vehicle at supersonic speeds are shown in figure 15. Variations of α, C_m, and L/D with C_L are shown for a test Mach number of 5. The lift curve may be seen to be very nearly linear. The vehicle is stable about the center of gravity at 55 percent of the length and is trimmed near maximum lift-drag ratio for the control settings indicated (lower flaps deflected 15° and elevons deflected -15°). The maximum lift-drag ratio, about 1.3, is essentially unchanged from that of the original 13° half-cone.

Figure 16 shows the variations with Mach number of the static longitudinal- and lateral-directional stability derivatives. It can be seen that the configuration was statically stable about the pitch and yaw axes throughout most of the test range and had positive dihedral effect. Two probable areas of difficulty to be noted are the nearly neutral pitch and yaw stability at a Mach number of about 0.9 and the high dihedral effect. This latter characteristic indicates the probability of a Dutch roll problem.

Measurements were made at transonic and supersonic speeds of the effectiveness of the pitch and yaw flaps and of the elevons. The measured moment-coefficient increments resulting from control deflections are shown in figures 17 and 18. Pitching-moment increments due to deflection of the lower pitch flaps and due to deflection of the elevons are shown in figure 17. It may be seen at the top of figure 17 that the pitch flaps provide large nose-down moments at subsonic and transonic speeds. At supersonic speeds the controls become relatively powerful when the deflection becomes positive relative to the stream. (The deflection angle is measured relative to the surface of the body.) The effectiveness of the elevons as pitch controls may be seen to decrease with increasing Mach number as is the case for most controls of this type. The indicated reversal at transonic speeds for an elevon deflection of 10° results from the effects of the pressure disturbance from the control on the top afterpart of the body. Yawing-moment and rolling-moment increments due to deflection of one yaw flap and differential deflection of the elevons are shown in figure 18. Again, the controls provide large moments in the subsonic and transonic speed ranges and their effectiveness decreases with increasing Mach number. (The elevon deflections for the data shown are $+20^\circ$ and -20° relative to a nominal position of -10° relative to the cone axis.) Only minor cross-coupling problems have been indicated in the test results obtained.

CONCLUDING REMARKS

The studies, thus far, of the half-cone type of lifting body have shown that, within limitations, this class of body shapes is useful for atmosphere entry requiring maneuvering capabilities. In the case of the low-fineness-ratio shapes, controllable flight through the transonic speed range would be difficult to achieve and the final landing would, of necessity, probably be by parachute or other auxiliary device. For the higher-fineness-ratio shapes, controllable flight throughout the speed range appears feasible and, with development, the capability of conventional landing is probably attainable.

Ames Research Center
National Aeronautics and Space Administration
Moffett Field, Calif., April 11, 1960

REFERENCES

1. Eggers, Alfred J., Jr., and Wong, Thomas J.: Re-entry and Recovery of Near-Earth Satellites, With Particular Attention to a Manned Vehicle. NASA MEMO 10-2-58A, 1958.

2. Bray, Richard S., Drinkwater, Fred J., III, and White, Maurice D.: A Flight Study of a Power-Off Landing Technique Applicable to Re-entry Vehicles. NASA TN D-323, 1960.

3. Weil, Joseph, and Matranga, Gene J.: Review of Techniques Applicable to the Recovery of Lifting Hypervelocity Vehicles. NASA TM X-334, 1960.

L
1
0
9
3

[redacted]

L-1093

BLUNT 30° HALF-CONE LIFTING BODY

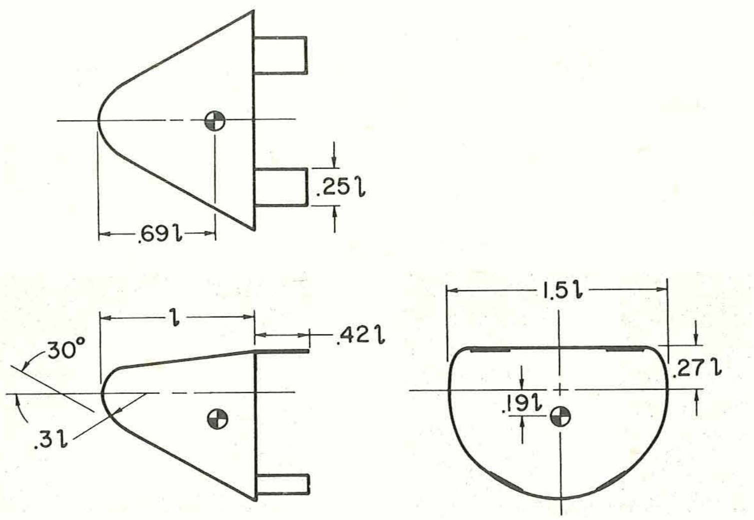

Figure 1

PERFORMANCE AND STATIC STABILITY OF 30° BLUNT HALF-CONE

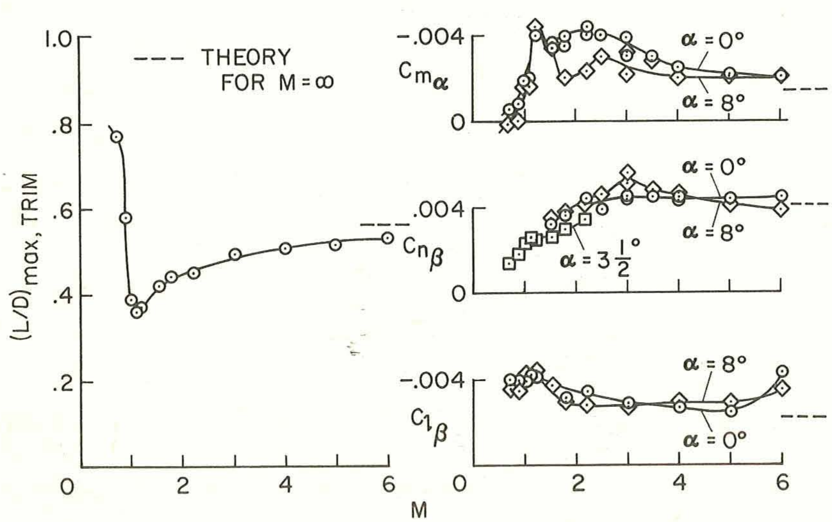

Figure 2

[redacted]

BLUNTED CONE SEGMENT

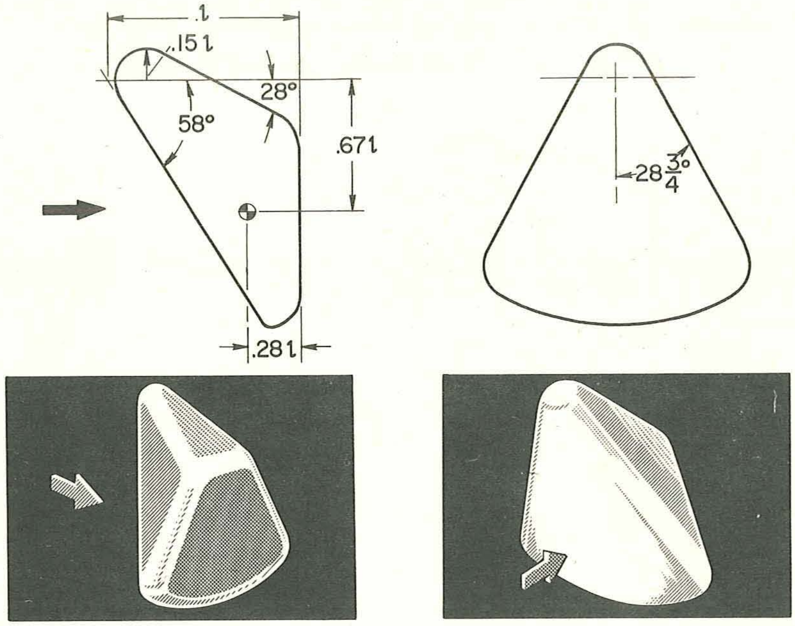

Figure 3

13° BLUNT HALF-CONE

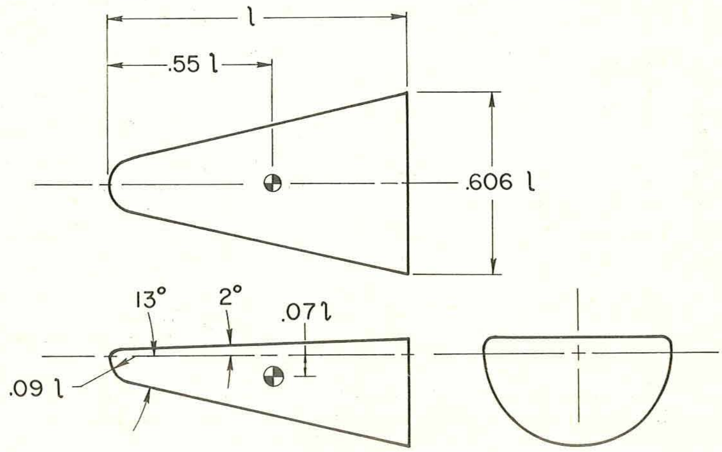

Figure 4

L1098

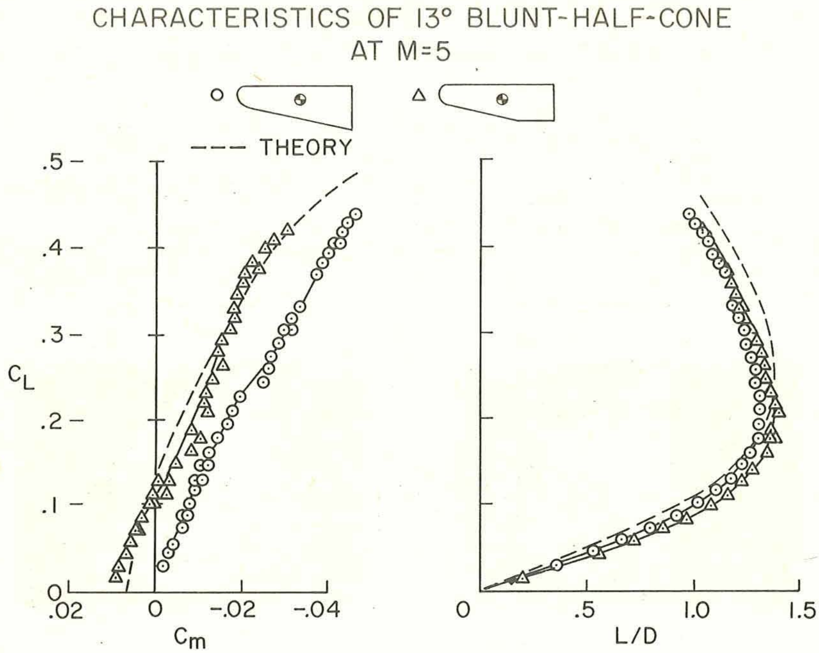

Figure 5

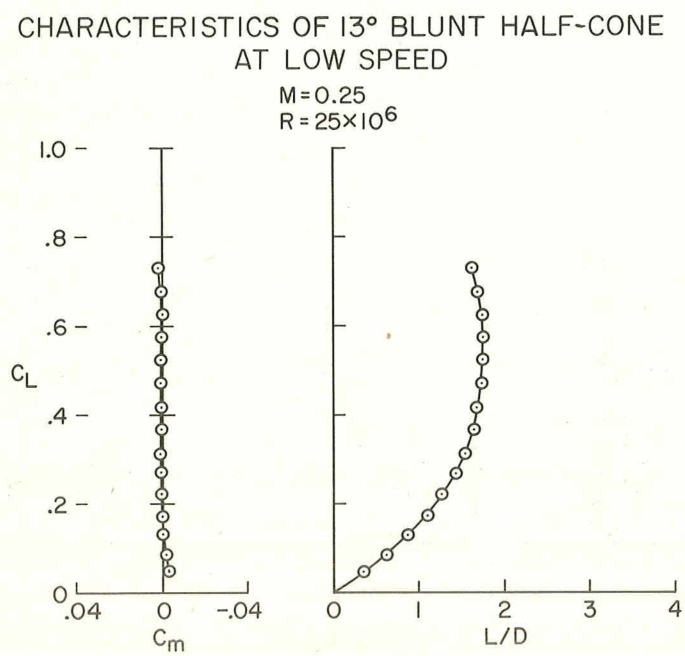

Figure 6

[redacted]

LIFTING BODIES INVESTIGATED

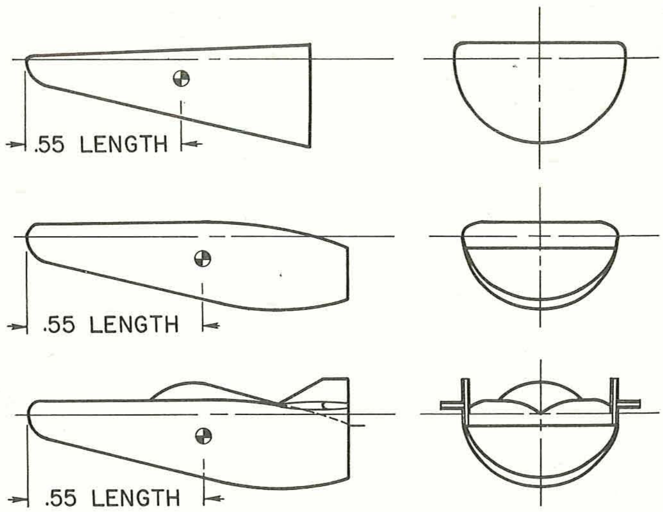

L
1
0
9
3

Figure 7

TYPICAL RESULTS AT M=0.25

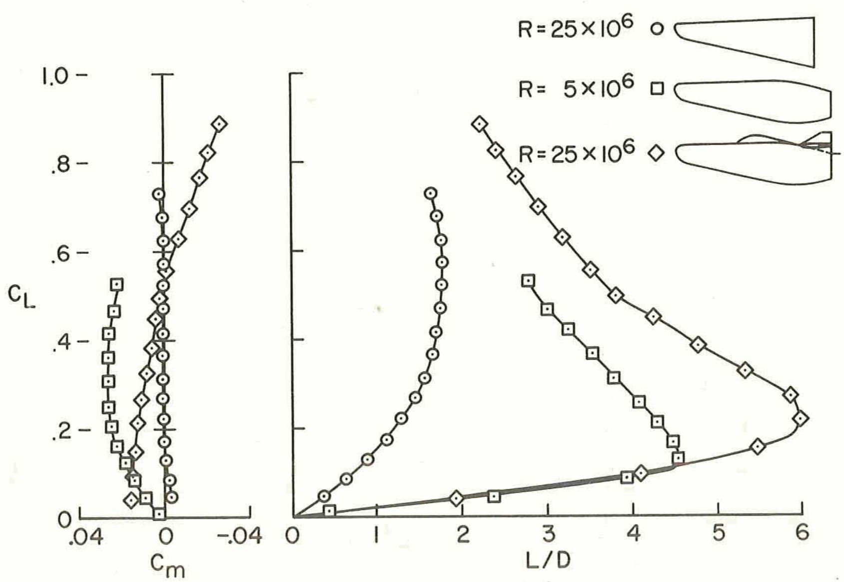

Figure 8

MODEL WITH SPHERICAL CANOPY

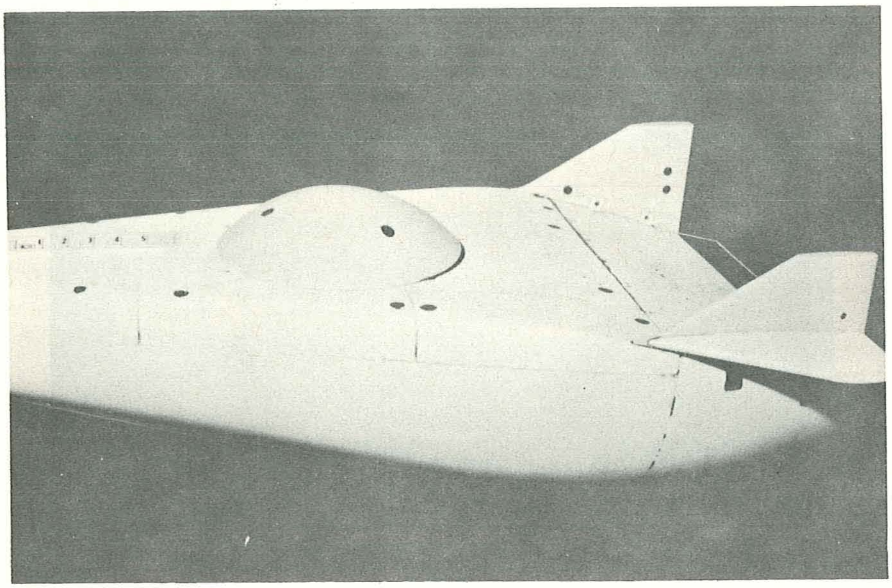

Figure 9

L1093

MODEL WITH FAIRED CANOPY

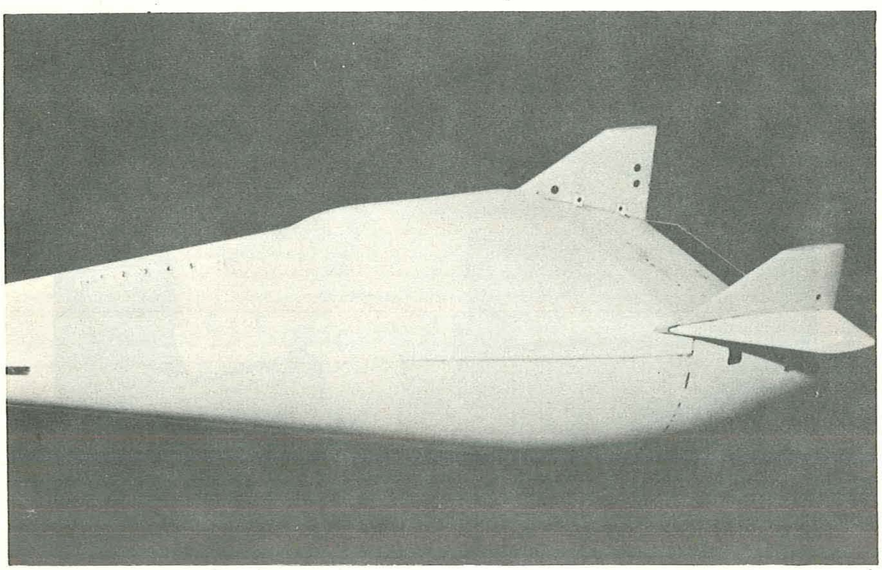

Figure 10

BODY WITH VERTICAL SURFACES AND CANOPY

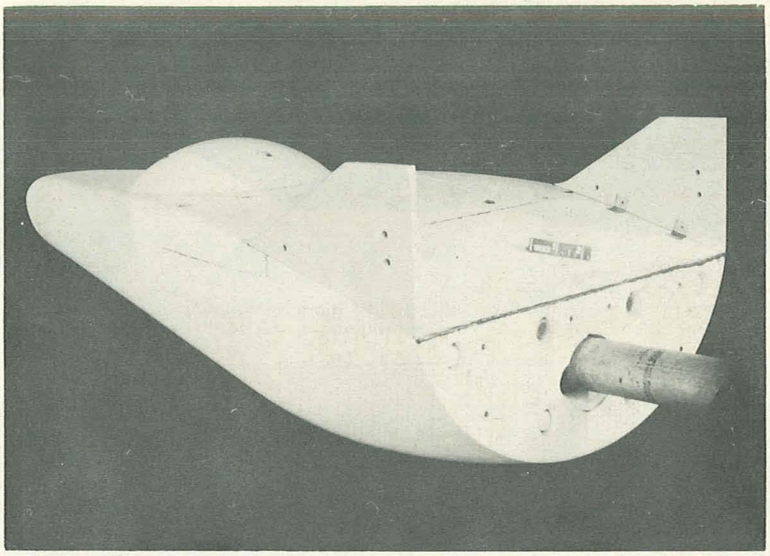

Figure 11

L 1 0 9 3

MODIFIED BODY WITH CONTROLS

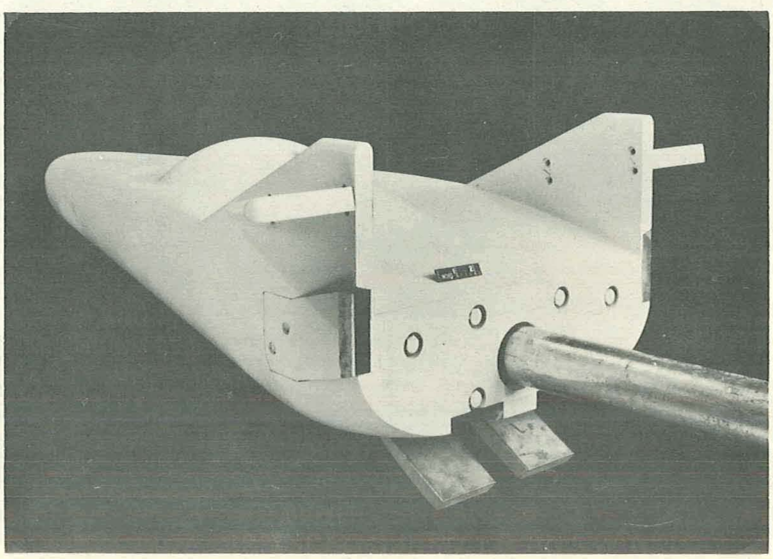

Figure 12

L1093

MODEL WITH LANDING GEAR

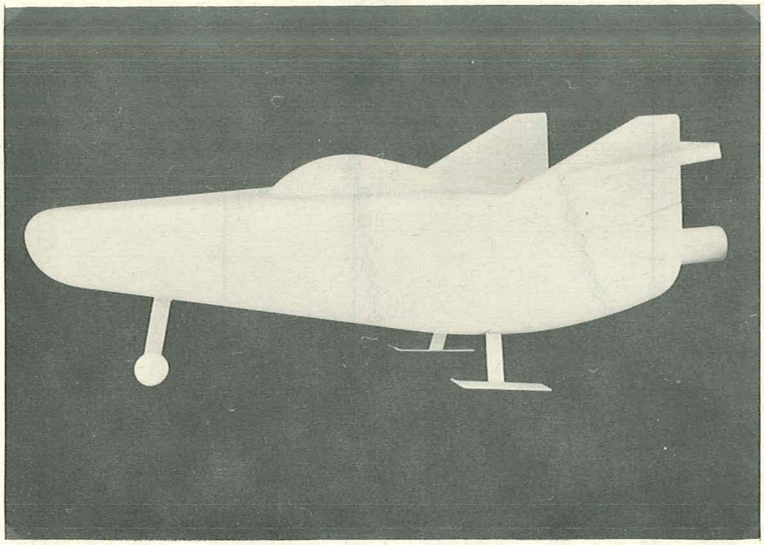

Figure 13

LOW-SPEED CHARACTERISTICS OF LANDING CONFIGURATION

$M = 0.25$
$R = 15 \times 10^6$

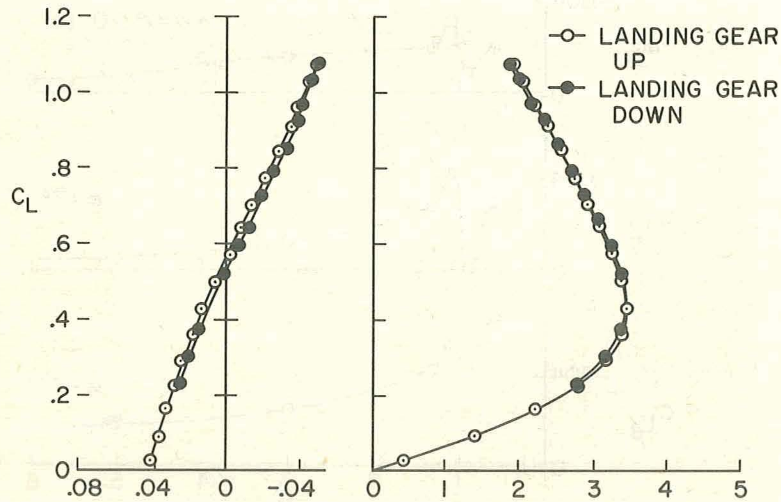

Figure 14

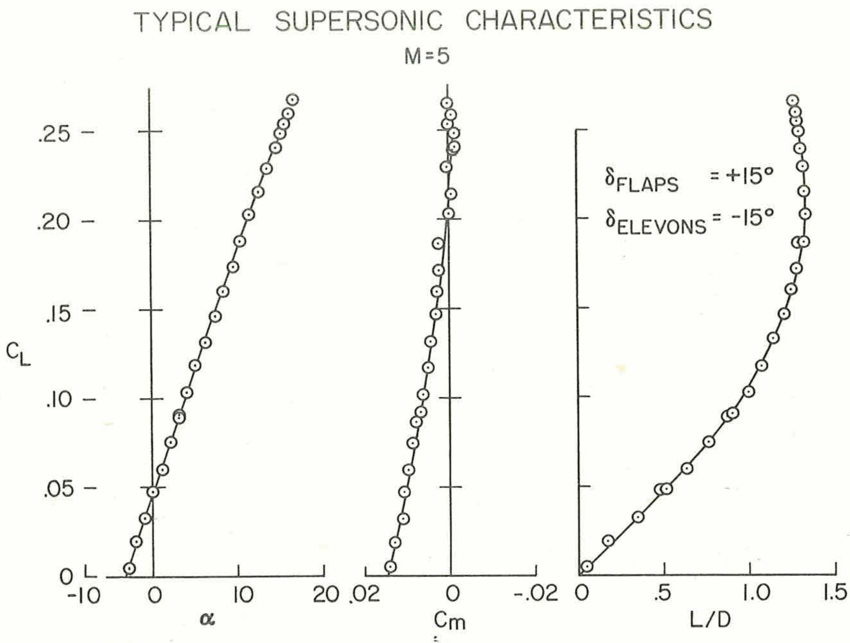

Figure 15

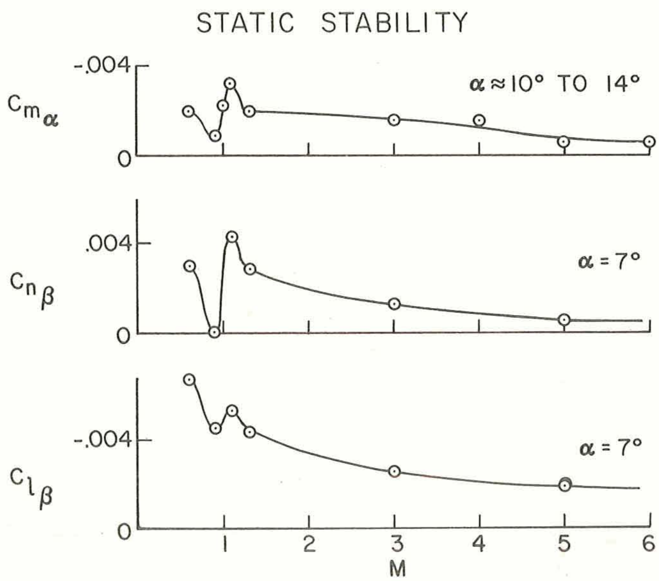

Figure 16

L1093

3V

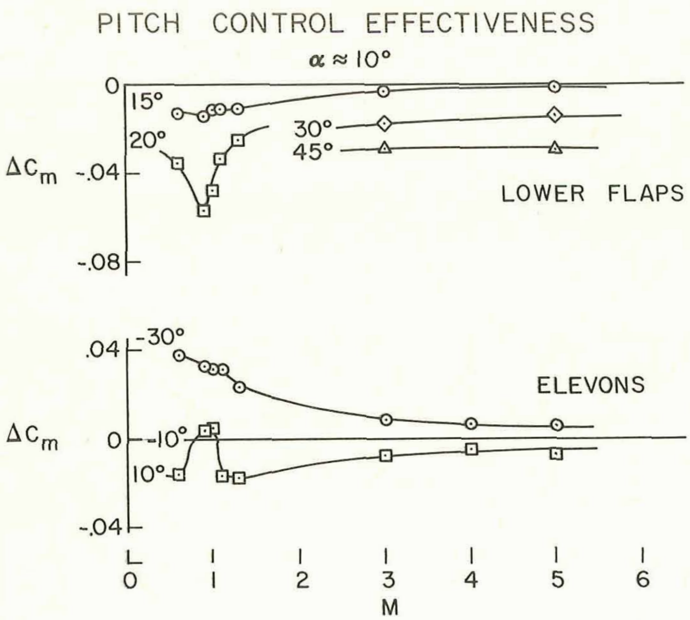

Figure 17

L
1
0
9
3

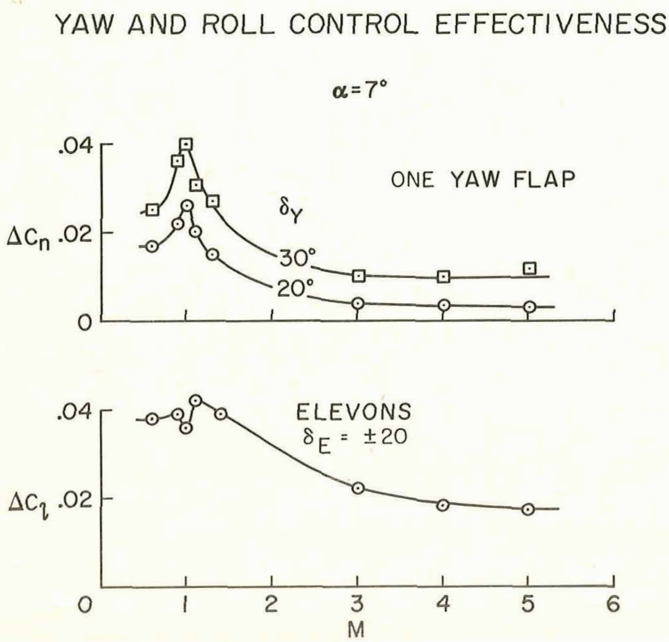

Figure 18

[redacted]

[redacted]